ELSEVIER

Hydrogenation of 1,3-butadiene on two ordered Sn/Pt(111) surface alloys

Haibo Zhao, Bruce E. Koel [*]

Department of Chemistry, University of Southern California, Los Angeles, CA 90089-0482, USA

Abstract

Adsorption and reaction of 1,3-butadiene (C_4H_6) on two ordered Pt–Sn surface alloys precovered with hydrogen adatoms were studied with the use of temperature-programmed desorption (TPD) mass spectroscopy and Auger electron spectroscopy (AES). The two alloys investigated were the (2×2)Sn/Pt(111) and $(\sqrt{3} \times \sqrt{3})$R30°-Sn/Pt(111) surface alloys, with 25 and 33% Sn alloyed in the surface layer, respectively, formed by vapor deposition of Sn onto a Pt(111) single crystal. Alloyed Sn opens a new hydrogenation reaction pathway compared with Pt(111). Butadiene hydrogenation by coadsorbed hydrogen occurs with 100% selectivity to liberate butene (C_4H_8) in reaction rate-limited peaks in TPD, and no deeper hydrogenation product (butane) was observed. The activation energy barrier for hydrogenation of strongly bound 1,3-butadiene is estimated to be 91 and 72 kJ/mol on the (2×2) and $(\sqrt{3} \times \sqrt{3})$R30° alloys, respectively. Butadiene conversion was highest on the (2×2) alloy, reaching 100% at high hydrogen precoverages. Strong site-blocking effects of preadsorbed H adatoms were observed for 1,3-butadiene chemisorption on both alloys under these conditions; butadiene chemisorption was eliminated by $\theta_H = 0.49$ ML on the (2×2) alloy and $\theta_H = 0.34$ ML on the $\sqrt{3}$ alloy. These studies addressing the influence of alloyed Sn on the reaction barrier to 1,3-butadiene hydrogenation and the effect of surface Sn concentration on hydrogenation activity provide observations of several novel phenomena and may aid in the development of heterogeneous catalysts to selectively remove dienes in alkene streams.
© 2004 Elsevier Inc. All rights reserved.

Keywords: 1,3-Butadiene; C_4H_6; hydrogen; H; hydrogenation; site blocking; Pt(111); Sn–Pt alloy; TPD

1. Introduction

The development of heterogeneous catalysts to selectively remove butadiene in C_4 alkene streams produced by steam cracking is of considerable interest. The ideal catalyst and process would convert butadiene selectively to butene but not lead to further hydrogenation of butene to butane. Various platinum surfaces, including supported catalysts [1–6] and single crystals [4,7–12], have been investigated regarding the hydrogenation of butadiene. Unfortunately, mixtures of butene isomers and butane apparently are usually produced over platinum catalysts.

Supported Pt–Sn bimetallic catalysts have been reported to be effective in the selective hydrogenation of diolefin impurities [13]. Generally, adding Sn to Pt catalysts used for

hydrocarbon conversion reactions results in decreased catalytic activity, increased selectivity for unsaturated hydrocarbon products, and reduced coking, which prolongs the lifetime of the catalyst. Specifically, several reports show that the presence of Sn in bimetallic Pt catalysts prevents alkene hydrogenation, which is important to the selective removal of diene impurities. Adding Sn to a supported Pt catalyst caused a dramatic decrease in catalytic activity for propene hydrogenation [14]. In addition, hydrogenation activity for ethylene and 1-hexene was inhibited on Pt–Sn/Al_2O_3 catalysts [15]. Although the reactivity of a Pt(111) single crystal increased slightly for ethylene hydrogenation when 0.1-ML Sn was added, it decreases quickly with further increase in the Sn coverage [16]. Experiments investigating coadsorption of hydrogen and ethylene on the $(\sqrt{3} \times \sqrt{3})$R30°-Sn/Pt(111) surface alloy under UHV conditions show that hydrogenation is completely inhibited by the combination of Sn with Pt(111) to form this alloy [17]. These results confirm that alloyed Sn

acts as an inhibitor to alkene hydrogenation. Other recent experiments have shown that chemisorbed 1,3-butadiene completely decomposes on both clean and H-precovered Pt(111) surfaces during TPD, with no hydrogenation reaction observed [18]. This presumably is due to the very strong bonding interactions between 1,3-butadiene and Pt(111). Previously we have shown in 1,3-butadiene chemisorption studies that alloying Sn with Pt(111) decreases this interaction, and the decomposition pathway is totally blocked on the (2 × 2) and ($\sqrt{3} \times \sqrt{3}$)R30°-Sn/Pt(111) surface alloys [19]. It is natural to inquire whether this reduced interaction between 1,3-butadiene and the Sn/Pt(111) surface alloys may lead to hydrogenation reactions in the presence of coadsorbed hydrogen.

In this paper we report on studies using temperature-programmed desorption (TPD) of adsorption and reaction of 1,3-butadiene on hydrogen-precovered (2 × 2)-Sn/Pt(111) and ($\sqrt{3} \times \sqrt{3}$)R30°-Sn/Pt(111) surface alloys. In particular, we address the influence of alloyed Sn on the reaction barrier to 1,3-butadiene hydrogenation and the effect of surface Sn concentration on hydrogenation activity.

2. Experimental

Experiments were performed in a three-level UHV chamber as described earlier [20]. The Pt(111) crystal (Atomergic; 10-mm diameter, 1.5 mm thick) was prepared by 1-keV Ar$^+$ ion sputtering and oxygen exposures (5×10^{-7} Torr O$_2$, at 900 K for 2 min) to give a clean spectrum with Auger electron spectroscopy (AES) and a sharp (1 × 1) pattern with low-energy electron diffraction (LEED).

We prepared the (2 × 2)Sn/Pt(111) and ($\sqrt{3} \times \sqrt{3}$)R30°-Sn/Pt(111) surface alloys by evaporating one monolayer of Sn onto the Pt(111) crystal surface and subsequently annealing the sample for 20 s to 1000 and 830 K, respectively. Sn is substitutionally incorporated primarily into the surface layer to form an ordered alloy or intermetallic compound with $\theta_{Sn} = 0.25$, with a composition and structure corresponding to the (111) face of a bulk Pt$_3$Sn crystal, and for the latter situation, $\theta_{Sn} = 0.33$, with a composition corresponding to a Pt$_2$Sn surface. These surface alloys are relatively "flat," but Sn atoms protrude 0.02 nm above the surface Pt plane at both surfaces [21]. In the (2 × 2) alloy, pure Pt three-fold sites are present, but no adjacent pure Pt three-fold sites exist. All pure Pt three-fold sites are eliminated on the ($\sqrt{3} \times \sqrt{3}$)R30° alloy, and only two-fold pure Pt sites are present. For brevity throughout this paper, we will refer to the (2 × 2)Sn/Pt(111) and ($\sqrt{3} \times \sqrt{3}$)R30°-Sn/Pt(111) surface alloys as the (2 × 2) and $\sqrt{3}$ alloys, respectively.

A Pt-tube doser was constructed, based on the design of Engel and Rieder [22], as a pyrolytic source of hydrogen atoms. The principal component is a bent Pt tube (1-mm o.d., 0.8-mm i.d.) into which a 0.1-mm-diameter hole was mechanically drilled. The tube was resistively heated to 1275 °C, and water cooling kept the adjacent Cu block

cold. The temperature of the Pt tube was directly measured with an optical pyrometer that was calibrated by the temperature of the Pt(111) crystal sample, as measured with a Cr/Al thermocouple. The estimated relative accuracy of the pyrometer reading was ±5 °C. The flux of H atoms obtained from this source operating at 800 °C with a background pressure rise in the chamber of 5×10^{-8} Torr was 3×10^{13} atoms cm^{-2} s^{-1}. We obtained this value by assuming that the initial sticking coefficient of H atoms on Pt(111) at 100 K was unity and using a calibration for the H coverage, θ_H, that was given by the hydrogen yield in TPD from the well-known decomposition of ethylene on Pt(111) [23].

H$_2$ (Matheson; 99.99%) was introduced via a variable leak valve (Granville–Phillips) into the Pt-tube doser. 1,3-Butadiene, C$_4$H$_6$ (Matheson; 99.5%), was used without additional purification. 1,3-Butadiene was exposed on the alloy surface by a microcapillary array doser connected to the gas line through a variable leak valve. All of the exposures reported here are given simply in terms of the background pressure in the UHV chamber as measured by an ion gauge. No attempt was made to correct for the flux enhancement of the doser or ion gauge sensitivity. The mass spectrometer in the chamber was used to check the purity of the gases during dosing.

For all TPD experiments, the heating rate was 3.6 K/s, and all exposures were made with the surface temperature at 100 K. AES measurements were made with a double-pass cylindrical mirror analyzer (CMA) and a modulation voltage of 4 eV. The electron gun was operated at 3-keV beam energy and 1.5-µA beam current. Coverages (θ_i) reported in this paper are referenced to the surface atom density of Pt(111) such that $\theta_{Pt} = 1.0$ ML is defined as 1.505×10^{15} cm^{-2}.

3. Results

Hydrogen adatoms were preadsorbed on the (2 × 2) alloy, and then adsorption and reaction of a monolayer of 1,3-butadiene (C$_4$H$_6$) on this surface at 100 K were investigated by TPD. An exposure of 0.24-L 1,3-butadiene was used, which produces a coverage of about two monolayers on the two clean alloy surfaces. Desorption spectra for 1,3-butadiene, C$_4$H$_6$ (54 amu); butene, C$_4$H$_8$ (56 amu); and H$_2$ (2 amu) obtained in these experiments are shown in Figs. 1–3, respectively. Several other masses, including butane, C$_4$H$_{10}$ (58 amu), were also monitored during heating in TPD, but no significant signals were detected in the TPD spectra.

Fig. 1 shows the thermal desorption of molecular 1,3-butadiene from the clean (bottom curve) and H-precovered (2 × 2) alloy surfaces. Desorption from the chemisorbed monolayer on the clean (2 × 2) alloy produces a wide peak centered at 334 K, which is consistent with our previous study [19]. There, we made an estimate of the desorption activation energy E_d of 88 kJ/mol by using the Redhead
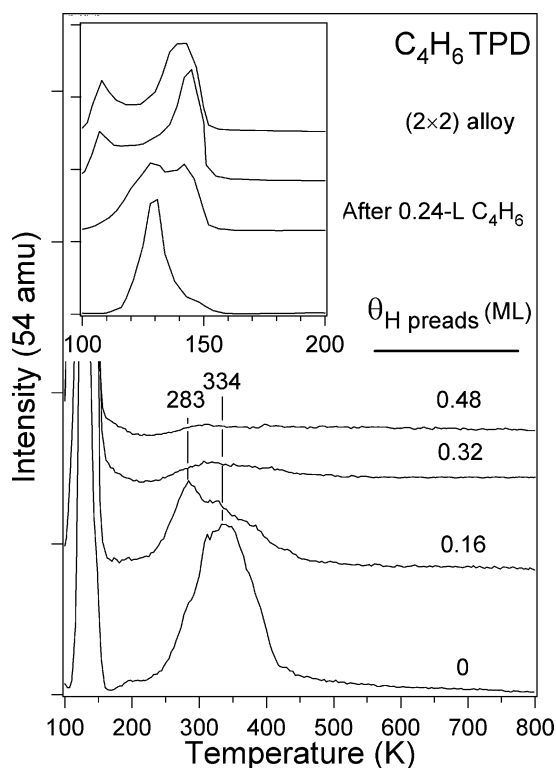
Fig. 1. 1,3-Butadiene, C_4H_6 TPD spectra after 0.24-L 1,3-butadiene exposures on the clean and H-precovered (2×2)Sn/Pt(111) alloy at 100 K.

Fig. 2. Butene, C_4H_8 TPD spectra after after 0.24-L 1,3-Butadiene exposures on the clean and H-precovered (2×2)Sn/Pt(111) alloy at 100 K.

method [24] and assuming first-order desorption kinetics with a preexponential factor of $10^{13}\,s^{-1}$.

Preadsorbed H adatoms reduce the amount of 1,3-butadiene desorption in this peak, and this peak disappears after preadsorption of 0.476-ML H. Desorption of the most strongly chemisorbed 1,3-butadiene is affected first by preadsorbed H. This is shown by the shift of the 1,3-butadiene desorption peak to a lower temperature and the appearance of a peak at 283 K ($E_d = 73$ kJ/mol) in the TPD spectra taken for 0.159-ML H.

The inset shows the low-temperature region of the desorption traces in Fig. 1 on an expanded scale. As shown in the inset, the desorption peak of physisorbed (second-layer) 1,3-butadiene shifts from 130 K on the clean (2×2) alloy to 140 K on the 0.476-ML H surface. Some clustering apparently occurs on the H-precovered surfaces, and low-temperature desorption onset characteristic of the multilayer appears near 105 K. One can calculate values of E_d of 33 and 35 kJ/mol for 1,3-butadiene adsorbed in the second layer on the clean and 0.476-ML H precovered (2×2) alloy, respectively.

Desorption of butene, C_4H_8, is shown in Fig. 2. This is a hydrogenation product produced by surface reactions. 1,3-Butadiene adsorption on the clean (2×2) alloy leads to a small amount of desorption (bottom curve) in a peak at 376 K. Because there is no coadsorption possible from H_2 in the background gas (i.e., H_2 does not dissociatively chemisorb on the (2×2) alloy under UHV conditions [25]), this must originate from hydrogenation reactions utilizing
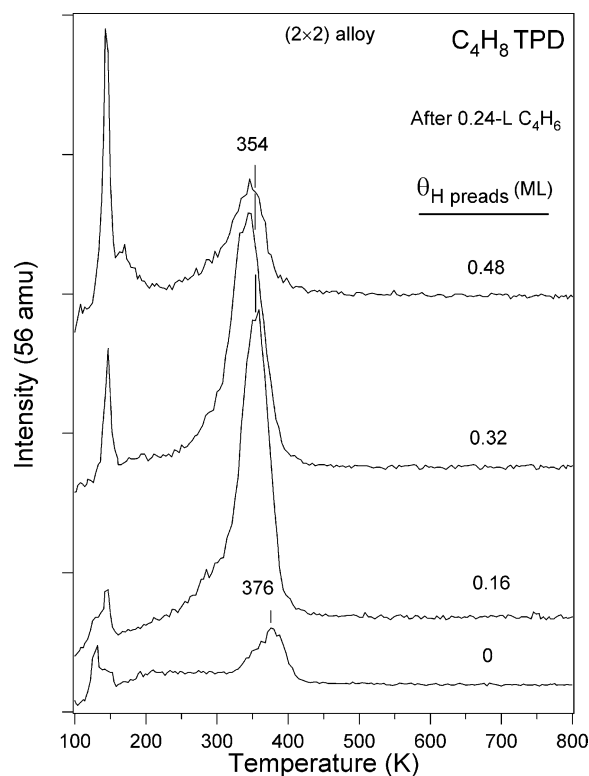
hydrogen liberated by 1,3-butadiene dehydrogenation. The amount of butene desorption is initially increased by H preadsorption and then decreased by the largest H precoverages. The decreased hydrogenation yield at high values of θ_H is due at least partially to the low coverage of 1,3-butadiene that results from the site-blocking effects of preadsorbed H. The butene desorption peak shifts down to 354 K ($E_d = 91$ kJ/mol) for 0.16-ML H and then to 345 K ($E_d = 89$ kJ/mol) for $\theta_H = 0.32$ and 0.48 ML. Because butene desorption is reaction-rate limited, as discussed below, this shift arises from faster reaction kinetics at higher θ_H.

Fig. 2 shows that some butene is produced below 200 K. The butene TPD peaks near 130 and 145 K have shapes similar to those of the low-temperature 1,3-butadiene desorption traces shown in the inset to Fig. 1, and thus these are TPD artifacts in the butene spectra. However, for $\theta_H = 0.32$ and 0.48 ML, the butene peak area at 145 K ($E_d = 36$ kJ/mol) increases significantly (and even a new peak arises at 170 K), whereas those for 1,3-butadiene do not, and so butene is indeed produced under these conditions. At these hydrogen precoverages, desorption of chemisorbed 1,3-butadiene near 300 K was nearly eliminated. This indicates that the low-temperature butene yield was due to facile hydrogenation of weakly adsorbed, π-bonded species.

Desorption of H_2 associated with these experiments is shown in Fig. 3. The bottom curve shows the H_2 yield from 1,3-butadiene dehydrogenation and decomposition on the
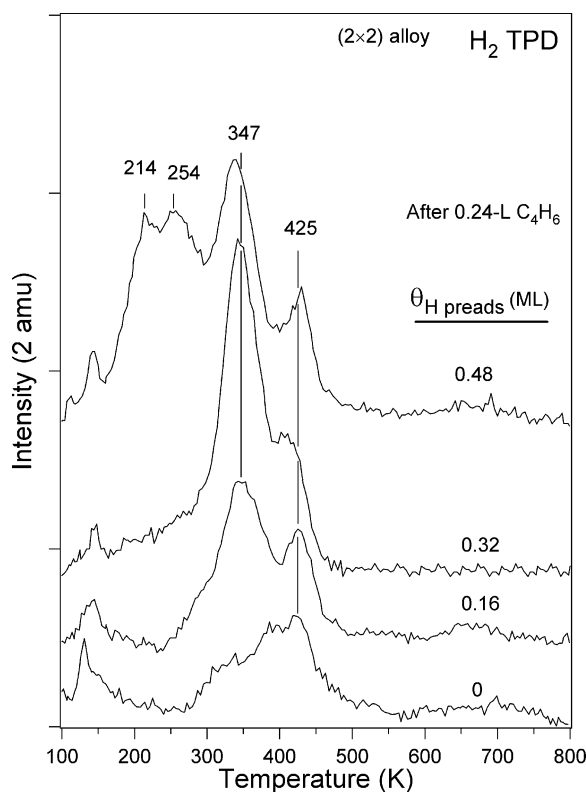
Fig. 3. H_2 TPD spectra after 0.24-L 1,3-butadiene exposures on the clean and H-precovered (2×2)Sn/Pt(111) alloy at 100 K.
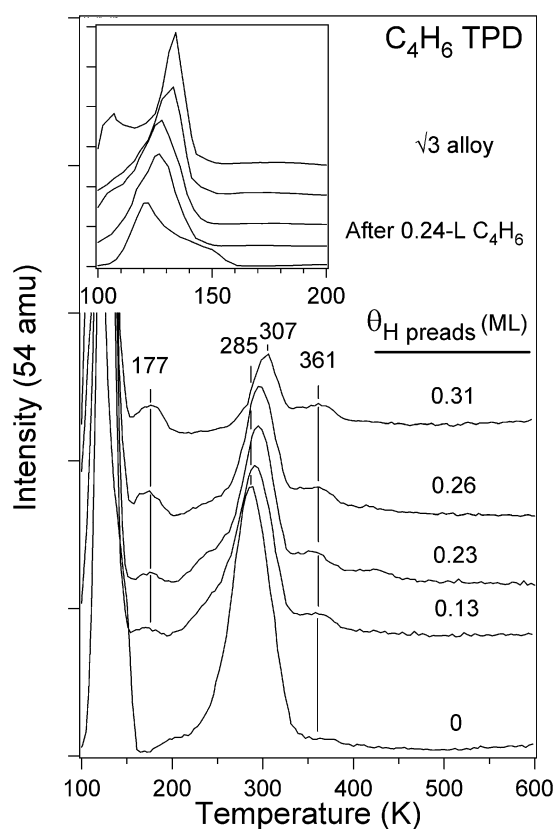

Fig. 4. 1,3-butadiene, C_4H_6 TPD spectra after 0.24-L 1,3-butadiene exposures on the clean and H-precovered $(\sqrt{3} \times \sqrt{3})$R30°-Sn/Pt(111) alloy at 100 K.

clean (2×2) alloy. This is consistent with previous studies [19] that showed only a small amount of dehydrogenation occurred. In such cases, it is difficult to distinguish between a small reactivity for the alloy and a small number of reactive defect sites. H preadsorption results in a new or larger H_2 desorption peak at 347 K ($E_d = 90$ kJ/mol) and a sharpening of the peak at 425 K ($E_d = 111$ kJ/mol). Increasing preadsorbed θ_H to 0.48 ML shifts the primary peak to a slightly lower temperature of 338 K and results in two new desorption peaks at 214 and 254 K. A comparison of these H_2 TPD spectra in Fig. 3 with those obtained after the same hydrogen exposure on the (2×2) alloy without 1,3-butadiene post-adsorption [26] establishes that the peaks at 214, 254, and 338–347 K in Fig. 3 are from desorption of preadsorbed H, and, furthermore, no shifts of these peaks were observed due to coadsorbed 1,3-butadiene. The peak at 425 K is similar to that observed in TPD for the decomposition of 1-butene and 2-butene at low coverages and 11 K higher than that from the full monolayers, on the (2×2) alloy [27]. Consistent with this H_2 desorption yield at 425 K, surface carbon was detected by AES after TPD experiments on the H precovered (2×2) alloy.

TPD experiments were also carried out after 0.24-L exposures of 1,3-butadiene on the clean and H-precovered $\sqrt{3}$ alloy at 100 K. Only 1,3-butadiene, C_4H_6 (54 amu); butene, C_4H_8 (56 amu); and H_2 (2 amu) were detected in TPD; these curves are shown in Figs. 4, 5, and 6, respectively.

Fig. 4 shows the influence of preadsorbed H on the desorption of molecular 1,3-butadiene from the $\sqrt{3}$ alloy. Chemisorbed 1,3-butadiene desorbs in a relatively narrow peak at 285 K (bottom curve) from the clean $\sqrt{3}$ alloy. This peak decreases in intensity with increasing H preadsorption and shifts up slightly to 307 K ($E_d = 79$ kJ/mol) on the $\sqrt{3}$ alloy with $\theta_H = 0.31$ ML. In addition, two new, weak desorption features arise at 177 and 361 K on the H precovered surfaces. Whereas the peak at 177 K ($E_d = 45$ kJ/mol) is probably from desorption of a weakly bound state of 1,3-butadiene in the monolayer, the peak at 361 K ($E_d = 93$ kJ/mol) is suggested to be from the dehydrogenation of some surface intermediate formed by hydrogenation reactions at lower temperatures. The intensity decrease with increasing θ_H occurs primarily from site-blocking effects of preadsorbed hydrogen on 1,3-butadiene chemisorption.

The inset in Fig. 4 highlights the H-induced changes in the desorption of physisorbed 1,3-butadiene. Desorption from the physisorbed, second layer shifts from 121 K on the clean $\sqrt{3}$ alloy to 134 K on the surface with $\theta_H = 0.31$ ML. This corresponds to a small increase in the desorption activation energy from 30 to 34 kJ/mol.

Fig. 5 shows butene TPD spectra that result from 1,3-butadiene hydrogenation reactions. On the clean $\sqrt{3}$ alloy, no butene desorption occurred. No coadsorbed hydrogen is possible from H_2 adsorption from the background [25], and
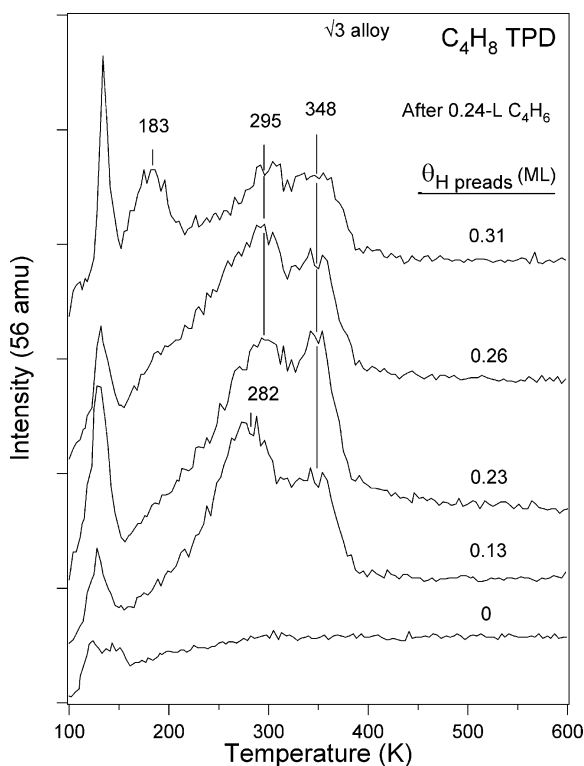
Fig. 5. Butene, C_4H_8 TPD spectra after 0.24-L 1,3-butadiene exposures on the clean and H-precovered $(\sqrt{3} \times \sqrt{3})R30°$-Sn/Pt(111) alloy at 100 K.

Fig. 6. H_2 TPD spectra after 0.24-L 1,3-butadiene exposures on the clean and H-precovered $(\sqrt{3} \times \sqrt{3})R30°$-Sn/Pt(111) alloy at 100 K.

no decomposition or self-hydrogenation occurs [19]. The low-temperature butene TPD peaks from the clean $\sqrt{3}$ alloy are thought to be TPD artifacts in the butene spectra, as discussed above. Preadsorbed H immediately leads to butene production and desorption, and two broad butene TPD peaks were observed at 282 and 348 K from the surface with $\theta_H = 0.13$ ML. The onset for butene desorption appears to be as low as 170 K ($E_d = 43$ kJ/mol). The peak at 282 K ($E_d = 72$ kJ/mol) shifts upward to 295 K ($E_d = 76$ kJ/mol) with increasing θ_H, but no large change occurs in the peak at 348 K ($E_d = 90$ kJ/mol). As occurred on the (2×2) alloy, for $\theta_H \geqslant 0.23$, butene is produced and desorbs near 134 K ($E_d = 34$ kJ/mol) because of facile hydrogenation of weakly adsorbed, π-bonded species. Increasing the H precoverage to 0.31 ML results in a new butene desorption peak at 183 K ($E_d = 46$ kJ/mol).

H_2 TPD spectra generated simultaneously in these experiments are shown in Fig. 6. The bottom trace of Fig. 6 was obtained after 1,3-butadiene adsorption on the clean $\sqrt{3}$ alloy. The result that there was no significant H_2 desorption is consistent with our previous study showing that 1,3-butadiene did not decompose on the $\sqrt{3}$ alloy during TPD [19]. There is a peak at 272 K ($E_d = 70$ kJ/mol) at $\theta_H = 0.13$, which shifts to 260 K ($E_d = 67$ kJ/mol) at $\theta_H = 0.31$ ML, and a peak at 217 K ($E_d = 55$ kJ/mol) for $\theta_H = 0.31$ ML. Signals below 200 K are derived from butadiene desorption and do not reflect H_2 desorption. The observation that no new H_2 TPD peaks arose and the close resemblance of the H_2 TPD peaks in Fig. 6 with those peaks obtained after the same H
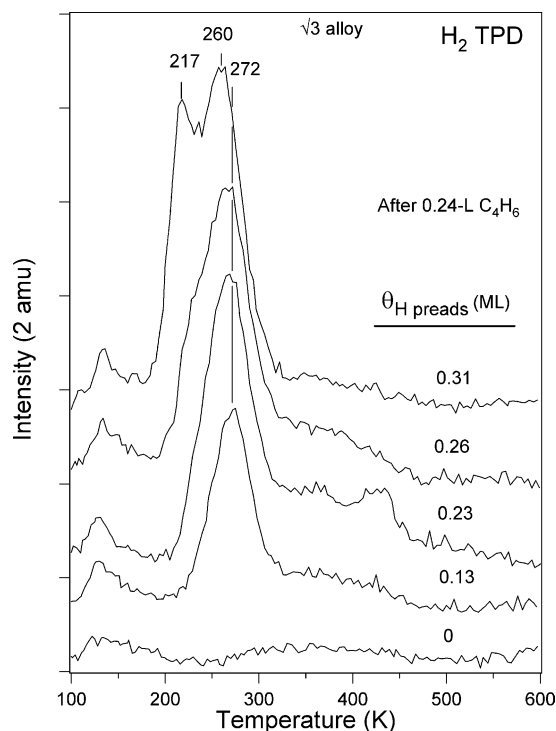
atom exposures without any subsequent 1,3-butadiene adsorption indicate that no 1,3-butadiene dehydrogenation or decomposition occurs under these conditions. AES measurements after each TPD experiment detect no surface carbon and thus give a consistent picture. Furthermore, coadsorbed 1,3-butadiene had no significant effect on the H_2 TPD spectra from H atom exposure.

In these experiments, we were unable to identify the nature of the butene molecules, that is, as 1-butene, *cis-* or *trans-*2-butene, or isobutene, that were desorbed as shown in Figs. 2 and 5. Previously, we studied the adsorption of 1-butene, *cis-*2-butene, and isobutene on Pt(111) and these two Sn/Pt(111) surface alloys [27]. We note that the conversion of the C_4H_8 TPD peak areas in Figs. 2 and 5 to the amount or coverage of desorbed butene is complicated by the fact that we cannot identify the butene isomers in TPD experiments. In general, this is a simple conversion determined by comparing the unknown TPD peak area to that from a calibrated yield of one of the butenes from Pt(111). However, if we do the conversion assuming that 1-butene is the desorbed product, and thus comparing directly with the yield of chemisorbed 1-butene from the 1-butene monolayer on Pt(111), we obtain about twice the yield that we would calculate by using 2-butene as the calibration. We obtained the butene yields reported below in Figs. 7 and 8 using 1-butene as the calibration.

Fig. 7 summarizes and quantifies the influence of preadsorbed H adatoms on the yields of products measured in the TPD data from the (2×2) alloy. We plot in Fig. 7, as a function of the H precoverage θ_H on the (2×2) alloy, the
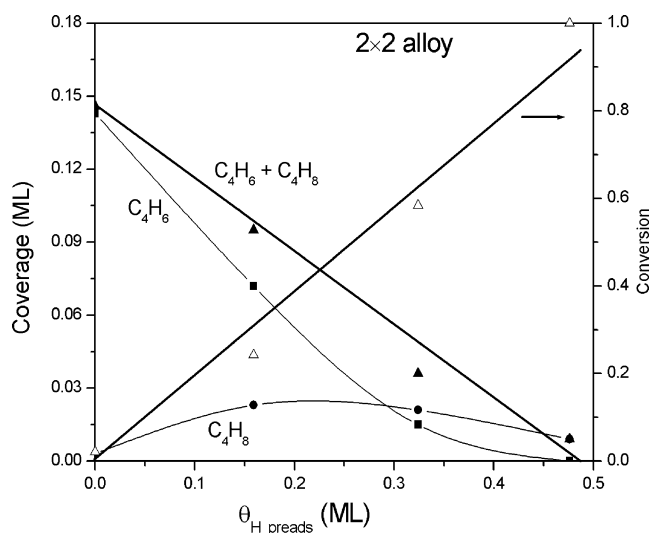
Fig. 7. Influence of H-adatom precoverage on the amount of 1,3-butadiene adsorption, desorption, and hydrogenation on the (2×2)Sn/Pt(111) alloy.

Fig. 8. Influence of H-adatom precoverage on the amount of 1,3-butadiene adsorption, desorption, and hydrogenation on the $(\sqrt{3} \times \sqrt{3})$R30°-Sn/Pt(111) alloy.

amount of reversibly chemisorbed 1,3-butadiene ($\theta_{C_4H_6}$), the amount of butene desorbed after formation by hydrogenation ($\theta_{C_4H_8}$), and the total amount of chemisorbed 1,3-butadiene ($\theta_{C_4H_6+C_4H_8}$). The conversion ($\theta_{C_4H_8}/\theta_{C_4H_6+C_4H_8}$) is also plotted on the right-hand axis.

The total coverage of chemisorbed 1,3-butadiene ($\theta_{C_4H_6+C_4H_8}$) is decreased, roughly linearly, by preadsorbed H, and we find that 1,3-butadiene chemisorption is eliminated when θ_H reaches 0.49 ML. This is a significant site-blocking influence exerted by H adatoms because 1,3-butadiene is potentially a strongly chemisorbed species. The other main effect that is observed is that the yield of butene from hydrogenation reactions increases strongly. The $\theta_{C_4H_8}$ curve increases from near zero on the clean alloy to a broad maximum near $\theta_H = 0.25$ ML. The decrease observed at larger θ_H values could easily be due simply to the decrease in the initial amount of 1,3-butadiene available for reaction. Of course, the amount of reversibly adsorbed 1,3-butadiene $\theta_{C_4H_6}$ decreases quickly with increasing θ_H because of the combined effects of increased site blocking and the propensity for hydrogenation reactions.

The conversion of 1,3-butadiene to butene increases almost linearly with increasing θ_H and reaches a value of 1.0 at $\theta_H = 0.47$ ML. But this hydrogenation is in competition with other processes on the surface during heating in TPD. Two H atoms are needed to hydrogenate one 1,3-butadiene molecule to produce one butene molecule. Although 1,3-butadiene is in surplus on the (2×2) alloy at small θ_H, some H atom recombination occurs to desorb H$_2$, and this competes with hydrogenation. On the (2×2) alloy with large θ_H, some 1,3-butadiene desorbs without being hydrogenated, even though H adatoms are oversupplied, and this competes with hydrogenation.

The influence of preadsorbed H on adsorption and hydrogenation of 1,3-butadiene on the $\sqrt{3}$ alloy is shown in Fig. 8. The site-blocking effects of preadsorbed H initially decrease
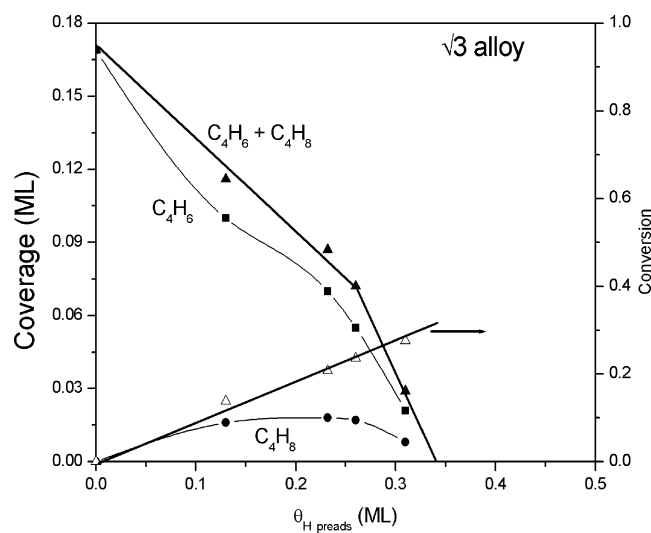
the total amount of chemisorbed 1,3-butadiene $\theta_{C_4H_6+C_4H_8}$ in a fashion very similar to that on the (2×2) alloy. For example, the total coverage is reduced to 0.085 ML on both alloys for $\theta_H = 0.23$ ML. However, for $\theta_H \geqslant 0.25$ ML, site blocking is much more effective on this alloy than on the (2×2) alloy and 1,3-butadiene chemisorption is completely blocked at $\theta_H = 0.34$ ML. The yield of desorbed butene $\theta_{C_4H_8}$ increases from zero on the clean alloy to a broad maximum with increasing H precoverage until, at $\theta_H = 0.26$ ML, it starts to decrease with additional θ_H because of the sharp decline in the amount of chemisorbed 1,3-butadiene available. Increasing θ_H also decreases the amount of desorbed 1,3-butadiene $\theta_{C_4H_6}$, but in this case the curve tracks much more closely the curve of the decrease in the total amount of chemisorbed 1,3-butadiene.

Preadsorbed H adatoms certainly increase the conversion of 1,3-butadiene to butene on the $\sqrt{3}$ alloy, almost linearly with increasing θ_H from a value of zero to 0.3 when $\theta_H = 0.34$ ML. However, this can be compared with a conversion of 65% on the (2×2) alloy at this value of θ_H. Conversion never climbs higher than 0.3 on the $\sqrt{3}$ alloy. As on the (2×2) alloy, hydrogenation on the $\sqrt{3}$ alloy is in competition with other processes on the surface during heating in TPD. H$_2$ desorption when $\theta_H < 2 \times \theta_{C_4H_6}$ indicates that hydrogenation competes with H recombination. Hydrogenation also competes with 1,3-butadiene desorption, which occurs even in cases of $\theta_H > 2 \times \theta_{C_4H_6}$.

4. Discussion

The addition of alloyed Sn in Pt surfaces weakens the bonding of hydrocarbons, such as alkenes and dienes, and this has been known for some time. The hydrogen coadsorption experiments reported here greatly extend our un-

derstanding of the influence of alloyed Sn on the chemistry and catalysis that occurs on Pt surfaces by revealing how this weakened bonding alters the influence of coadsorbed hydrogen on adsorption, desorption, and hydrogenation rates.

Blocking of strong adsorption sites by preadsorbed H adatoms on Pt(111) has been reported previously [28]. We also observed this H adatom site-blocking effect for 1,3-butadiene adsorption on H-precovered Pt(111) and have proposed why this could be a general phenomenon for other hydrocarbons [18]. Such a site-blocking effect of preadsorbed H was also observed in this work for 1,3-butadiene chemisorption on both Sn/Pt(111) surface alloys. What is interesting is to realize how alloyed Sn increases the importance of this effect, that is, why much smaller amounts of hydrogen are needed to block chemisorption on the alloy surfaces. Even though the monolayer saturation coverage of chemisorbed 1,3-butadiene (0.15 ML) is nearly the same on Pt(111) and the (2×2) and $\sqrt{3}$ alloys, the amount of preadsorbed hydrogen needed to completely block 1,3-butadiene chemisorption on Pt(111) is $\theta_H = 0.91$ ML, but $\theta_H = 0.49$ and 0.34 ML on the (2×2) and $\sqrt{3}$ alloy, respectively. The implications of this behavior are clear. One H adatom per unit cell on Pt(111), adsorbed in a three-fold hollow site, produces a saturation coverage of 1 ML. Each Pt at the surface has a nearest-neighbor H adatom, and this evidently passivates the surface against additional H atom uptake and strong 1,3-butadiene chemisorption. On the (2×2) alloy, two H adatoms per unit cell, adsorbed in pure Pt, 3-fold hollow sites, produces a saturation coverage of 0.5 ML. The two H adatoms occupy one *fcc* and one *hcp* site, with each Pt at the surface having a nearest-neighbor H adatom, and one Pt per unit cell having two nearest-neighbor H adatoms. This evidently passivates the surface against additional H atom uptake and strong 1,3-butadiene chemisorption. Only one H adatom per unit cell on the $\sqrt{3}$ alloy is required for this passivation. Each H adatom is presumed to be adsorbed in a pure Pt, 2-fold bridge site at the center of each unit cell to produce a saturation coverage of 0.33 ML. Each Pt at the surface has a nearest-neighbor H adatom. Obviously, electronic structure calculations are needed to validate and establish such proposals, but we hope these arguments stimulate such work.

Another significant difference in the chemistry of coadsorbed hydrogen on Pt(111) compared with that on the two Sn/Pt(111) alloy surfaces is the reactivity for hydrogenating 1,3-butadiene. On Pt(111), chemisorbed 1,3-butadiene is completely irreversibly adsorbed and completely decomposes to liberate H_2 and form surface carbon [19]. This chemistry is unaffected by coadsorbed hydrogen, and, specifically, no butene desorption occurs [18]. This may indicate that dehydrogenation occurs more easily on Pt(111) than hydrogenation, or possibly that the hydrogenation barrier of strongly chemisorbed 1,3-butadiene is larger than the H_2 desorption barrier for coadsorbed H adatoms. The adsorption energy of 1,3-butadiene is decreased on the two

Sn/Pt(111) alloy surfaces, and alloying has an even stronger affect on 1,3-butadiene decomposition; that is, decomposition is nearly eliminated on the (2×2) alloy and completely eliminated on the $\sqrt{3}$ alloy [19]. This is due to an increase in the C–H bond breaking barrier. On both alloys containing preadsorbed hydrogen, a significant amount of butene desorption from the hydrogenation of 1,3-butadiene occurs. This activity is much larger on the (2×2) alloy, and 100% conversion of 1,3-butadiene to butene is achieved at high values of θ_H (near 0.5 ML).

We did not determine which butene isomer (1-butene, *cis*- or *trans*-2-butene, or isobutene) was produced in our TPD experiments. Both 1-butene and *cis*-2-butene desorb at low coverage on the (2×2) alloy at 270 K and on the $\sqrt{3}$ alloy below 220 K [27]. Thus, butene desorption at temperatures higher than those in Figs. 2 and 5 is rate-limited by hydrogenation reactions. Butene produced at 170–183 K by hydrogenation of weakly adsorbed, π-bonded species appears to be reaction rate limited, but butene evolution at 140–145 K occurs at about the temperature at which butene desorbs from physisorbed layers, and so we do not distinguish the limiting kinetics in this case.

Reaction rate-limited butene desorption peaks in TPD can be used to estimate the hydrogenation reaction barrier E_a for strongly chemisorbed 1,3-butadiene on the two surface alloys (i.e., $E_d = E_a$). The single butene desorption peak at 354 K on the (2×2) alloy with $\theta_H = 0.16$-ML H corresponds to a hydrogenation reaction barrier of $E_a = 91$ kJ/mol. On the $\sqrt{3}$ alloy with $\theta_H = 0.13$-ML H, the two butene desorption peaks at 282 and 348 K correspond to $E_a = 72$ and 90 kJ/mol, respectively.

Surface-bound butenyl groups, either 1-butenyl $(-CH_2CH_2CH=CH_2)$ or 2-butenyl $(-CH(CH_3)CH=CH_2)$, are considered to be reaction intermediates in 1,3-butadiene hydrogenation on Pt surfaces at high pressure [12]. Although there is no spectroscopic evidence at this time for butenyl groups on H-precovered Sn/Pt(111) alloys, it is reasonable to assume that hydrogenation occurs on these alloys through such intermediates. Our TPD data provide some clues that an additional path exists on the $\sqrt{3}$ alloy. We observed two reaction-rate-limited butene desorption peaks and a high-temperature 1,3-butadiene desorption peak. In previous studies, surface-bound ethyl groups (CH_3CH_2-) were observed to produce ethylene and ethane on the $\sqrt{3}$ alloy at 376 K through self-hydrogenation [29]. Surface-bound butenyl groups would be expected to react via β-H elimination to produce butadiene and butane simultaneously. On the H-precovered $\sqrt{3}$ alloy, all hydrogen desorbs before 330 K and thus is not available for hydrogenation reactions at higher temperatures. This strongly suggests that the butene desorption peak at 348 K is from self-hydrogenation of surface-bound butenyl groups. This conclusion is also supported by observation of 1,3-butadiene desorption at 361 K.
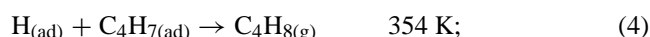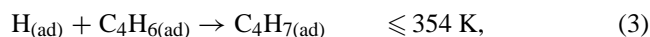
Apparently, high coverages of H adatoms are able to hydrogenate weakly bound, π-bonded 1,3-butadiene species on both alloys. On the $\sqrt{3}$ alloy at $\theta_H = 0.31$ ML, a particu-

larly weakly bound state of H adatoms exists on the surface, and these species recombine and desorb as H_2 at 217 K, as presented in Fig. 6. These species cause a new, weakly bound, π-bonded 1,3-butadiene species to form that desorbs at 177 K, as shown in Fig. 4, and are implicated in the hydrogenation of these 1,3-butadiene species to form butane, which desorbs in a new peak at 183 K.
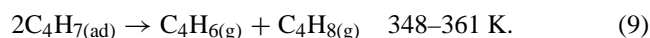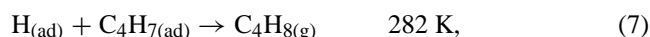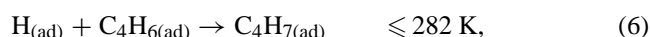
Both Sn/Pt(111) surface alloys have 100% selectivity for the conversion of 1,3-butadiene to butene versus butane; butane was never detected as a desorbed product in these experiments. This observation is promising for applications of Sn–Pt bimetallic catalysts in the selective removal of dienes from alkene feeds. This selectivity is caused in part by the decrease in the butene adsorption energy when Sn is alloyed with Pt(111). Butene desorbs before any hydrogenation reaction occurs because the butene desorption activation energy barrier is lower than that of the hydrogenation reaction barrier, based on our previous studies of ethylene hydrogenation [17].

Reactions on the two Sn/Pt(111) surface alloys at low θ_H can be summarized by the following scheme:

(2 × 2) alloy

$$C_4H_{6(ad)} \rightarrow C_4H_{6(g)} \qquad 283 \text{ K}, \qquad (1)$$

$$2H_{(ad)} \rightarrow H_{2(g)} \qquad 347 \text{ K}, \qquad (2)$$

$$H_{(ad)} + C_4H_{6(ad)} \rightarrow C_4H_{7(ad)} \qquad \leqslant 354 \text{ K}, \qquad (3)$$

$$H_{(ad)} + C_4H_{7(ad)} \rightarrow C_4H_{8(g)} \qquad 354 \text{ K}; \qquad (4)$$

$\sqrt{3}$ alloy

$$2H_{(ad)} \rightarrow H_{2(g)} \qquad 272 \text{ K}, \qquad (5)$$

$$H_{(ad)} + C_4H_{6(ad)} \rightarrow C_4H_{7(ad)} \qquad \leqslant 282 \text{ K}, \qquad (6)$$

$$H_{(ad)} + C_4H_{7(ad)} \rightarrow C_4H_{8(g)} \qquad 282 \text{ K}, \qquad (7)$$

$$C_4H_{6(ad)} \rightarrow C_4H_{6(g)} \qquad 285 \text{ K}, \qquad (8)$$

$$2C_4H_{7(ad)} \rightarrow C_4H_{6(g)} + C_4H_{8(g)} \quad 348–361 \text{ K}. \qquad (9)$$

Although $\theta_{C_4H_6}$ is larger on the $\sqrt{3}$ alloy than on the (2 × 2) alloy at the same value of θ_H, the 1,3-butadiene conversion to butene is smaller on the $\sqrt{3}$ alloy because the H_2 desorption activation energy on the $\sqrt{3}$ alloy is a little smaller than that for 1,3-butadiene. This causes more of the coadsorbed H to recombine and desorb as H_2. On the (2 × 2) alloy, recombinative H_2 and 1,3-butadiene desorption have similar activation energies, and this results in more extensive hydrogenation reactions. These arguments lead to the conclusion that hydrogenation reactions are maximized when 1,3-butadiene and recombinative H_2 desorption have the same activation energies. In practical catalysts, this synergy might be exploited by control of the Sn concentration in the supported Sn–Pt catalysts.

5. Conclusions

Alloying Sn with Pt(111) opens a new pathway for hydrogenation, compared with chemistry on Pt(111), to selec-

tively produce butene during heating of coadsorbed layers of H and 1,3-butadiene in TPD. This hydrogenation reaction was observed on both of the two ordered Sn/Pt(111) surface alloys investigated. No further hydrogenation reactions producing butane were observed. We estimated the activation energy barriers to hydrogenation of strongly chemisorbed 1,3-butadiene to be 91 and 72 kJ/mol on the (2 × 2) alloy and $\sqrt{3}$ alloys, respectively, by considering the butene desorption that occurs at 354 and 282 K. 1,3-Butadiene hydrogenation occurs in competition with 1,3-butadiene desorption and hydrogen adatom recombination to desorb H_2, and the relative rates vary with θ_H and depend on the alloy surface. The highest conversion from 1,3-butadiene to butene was observed on the (2 × 2) alloy, and this is likely due to the nearly matching desorption activation energies of H_2 and 1,3-butadiene on the (2 × 2) alloy, compared with that on the $\sqrt{3}$ alloy. This leads to high coverages of both reactants at the highest temperatures, and this synergy might be exploited in practical catalyst by control of the Sn concentration.

Hydrogenation of 1,3-butadiene presumably proceeds through surface-bound butenyl groups as intermediates on both alloys to produce reaction-rate-limited butene desorption at 282–354 K. In addition, on the $\sqrt{3}$ alloy, self hydrogenation of surface butenyl groups also occurs during heating in TPD and produces butene desorption at 348 K. We also observed a small amount of facile, low-temperature hydrogenation of weakly bound, π-bonded 1,3-butadiene to butene, which desorbed in reaction rate-limited peaks below 200 K corresponding to a hydrogenation activation barrier of 46 kJ/mol.

Site-blocking effects by H adatoms on 1,3-butadiene adsorption were observed on both of the two Sn/Pt(111) alloys, as we saw previously on Pt(111). However, the amount of preadsorbed hydrogen needed to complete block 1,3-butadiene chemisorption on the two alloys was much less than that needed on Pt(111), that is, $\theta_H = 0.49$ and 0.34 ML on the (2 × 2) and $\sqrt{3}$ alloy, respectively, compared with $\theta_H = 0.91$ on Pt(111). We propose a simple model for hydrogen adsorption to explain these changes.

References

[1] G.C. Bond, G. Webb, P.B. Wells, J.M. Winterbottom, J. Catal. 1 (1962) 74.
[2] G.C. Bond, G. Webb, P.B. Wells, J.M. Winterbottom, J. Chem. Soc. A (1965) 3218.
[3] P.B. Wells, A.J. Bates, J. Chem. Soc. A (1968) 3064.

[4] C.M. Pradier, E. Margot, Y. Berthier, J. Qudar, Appl. Catal. 43 (1988) 177.

[5] M. Primet, M. El Azhar, M. Guenin, Appl. Catal. 58 (1990) 241.

[6] A. Sarkany, G. Stefler, J.W. Hightower, Appl. Catal. A: Gen. 127 (1995) 77.

[7] J. Massardier, J.C. Bertolini, P. Ruiz, P. Delichere, J. Catal. 112 (1988) 21.

[8] J. Qudar, S. Pinol, Y. Berthier, J. Catal. 107 (1987) 434.

[9] C.M. Pradier, E. Margot, Y. Berthier, J. Qudar, Appl. Catal. 31 (1987) 243.

[10] T. Ouchaib, J. Massardier, A. Renouprez, J. Catal. 119 (1989) 517.

[11] C.M. Pradier, Y. Berthier, J. Catal. 129 (1991) 356.

[12] C. Yoon, M.X. Yang, G.A. Somorjai, Catal. Lett. 46 (1997) 37.

[13] D.F. Rohr, D.M. Haskell, F.M. Brinkmeyer, Eur. Pat. Appl. EP 211381 A1 19870225 (1987).

[14] M. Galvagno, P. Staiti, P. Antonucci, A. Donato, R. Pietropaolo, J. Chem. Soc., Faraday Trans. 79 (1983) 2605.

[15] A. Palazov, Ch. Bonev, D. Shopov, G. Lietz, A. Sárkány, J. Völter, J. Catal. 103 (1987) 249.

[16] Y. Park, F.H. Ribeiro, G.A. Somorjai, J. Catal. 178 (1998) 66.

[17] H. Zhao, B.E. Koel, Langmuir 21 (2005) 971.

[18] H. Zhao, B.E. Koel, Surf. Sci., submitted for press.

[19] H. Zhao, B.E. Koel, Surf. Sci. 572 (2004) 261.

[20] H. Zhao, J. Kim, B.E. Koel, Surf. Sci. 538 (2003) 147.

[21] S.H. Overbury, D.R. Mullins, M.T. Paffett, B.E. Koel, Surf. Sci. 254 (1991) 45.

[22] T. Engel, K.H. Rieder, in: G. Höhler (Ed.), Structural Studies of Surfaces, vol. 91, Springer, Berlin, 1982, p. 55.

[23] R.G. Wndham, M.E. Bartram, B.E. Koel, J. Phys. Chem. 92 (1988) 2862.

[24] P.A. Redhead, Vacuum 12 (1962) 203.

[25] M.T. Paffett, S.C. Gebhard, R.G. Windham, B.E. Koel, J. Phys. Chem. 94 (1990) 6831.

[26] H. Zhao, PhD thesis, University of Southern California.

[27] Y. Tsai, B.E. Koel, J. Phys. Chem. B 101 (1997) 2895.

[28] C. Lutterloh, J. Biener, K. Pöhlmann, A. Schenk, J. Küppers, Surf. Sci. 352 (1996) 133.

[29] H. Zhao, B.E. Koel, Catal. Lett. 99 (2005) 27.